Received: 21 March 2023 | Accepted: 2 April 2023

DOI: 10.1002/prp2.1091

ORIGINAL ARTICLE

Rapamycin treatment increases survival, autophagy biomarkers and expression of the anti-aging klotho protein in elderly mice

Kitti Szőke[1] | Beáta Bódi[2] | Zoltán Hendrik[3] | Attila Czompa[1] | Alexandra Gyöngyösi[1,4] | Donald David Haines[5] | Zoltán Papp[2,6] | Árpád Tósaki[1,7] | István Lekli[1,4]

[1]Department of Pharmacology, Faculty of Pharmacy, University of Debrecen, Debrecen, Hungary

[2]Division of Clinical Physiology, Faculty of Medicine, University of Debrecen, Debrecen, Hungary

[3]Institute of Forensic Medicine, Faculty of Medicine, University of Debrecen, Debrecen, Hungary

[4]Institute of Healthcare Industry, University of Debrecen, Debrecen, Hungary

[5]Advanced Biotherapeutics, London, UK

[6]HAS-UD Vascular Biology and Myocardial Pathophysiology Research Group, Hungarian Academy of Sciences, Budapest, Hungary

[7]ELKH-DE Pharmamodul Research Team, University of Debrecen, Debrecen, Hungary

Correspondence
István Lekli, Department of Pharmacology, Faculty of Pharmacy, University of Debrecen, Debrecen, Hungary, Institute of Healthcare Industry, University of Debrecen, Debrecen, Hungary.
Email: lekli.istvan@pharm.unideb.hu

Funding information
Emberi Erőforrás Fejlesztési Operatív Program, Grant/Award Number: EFOP-3.6.3-VEKOP-16-2017-00009 and EFOP-3.6.1-16-2016; Gazdaságfejlesztési és Innovációs Operatív Program, Grant/Award Number: GINOP-2.3.4-15-2020-00008; Nemzeti Kutatási Fejlesztési és Innovációs Hivatal, Grant/Award Number: NKFI-143360; Thematic Excellence Program, Grant/Award Number: TKP2020-IKA-04

Abstract

Previous investigations have demonstrated that treatment of animals with rapamycin increases levels of autophagy, which is a process by which cells degrade intracellular detritus, thus suppressing the emergence of senescent cells, whose pro-inflammatory properties, are primary drivers of age-associated physical decline. A hypothesis is tested here that rapamycin treatment of mice approaching the end of their normal lifespan exhibits increased survival, enhanced expression of autophagic proteins; and klotho protein—a biomarker of aging that affects whole organism senescence, and systemic suppression of inflammatory mediator production. Test groups of 24-month-old C57BL mice were injected intraperitoneally with either 1.5 mg/kg/week rapamycin or vehicle. All mice administered rapamycin survived the 12-week course, whereas 43% of the controls died. Relative to controls, rapamycin-treated mice experienced minor but significant weight loss; moreover, nonsignificant trends toward decreased levels of leptin, IL-6, IL-1β, TNF-α, IL-1α, and IGF-1, along with slight elevations in VEGF, MCP-1 were observed in the blood serum of rapamycin-treated mice. Rapamycin-treated mice exhibited significantly enhanced autophagy and elevated expression of klotho protein, particularly in the kidney. Rapamycin treatment also increased cardiomyocyte

Abbreviations: BCA, Bicinchoninic acid; BSA, bovine serum albumin; EDTA, Ethylenediamine tetraacetic acid; hsp 70, heat shock protein 70; IGF-1, insulin/insulin-like growth factor-1; IGF-1, Insulin-like growth factor 1; IL-1α, Interleukin-1 alpha; IL-1β, Interleukin 1 beta; IL-6, Interleukin-6; MCP-1, Monocyte chemoattractant protein-1; NF-kB, factor nuclear factor-kappa beta; NP-40, nonionic polyoxyethylene surfactant; PBS, Phosphate-buffered saline; PEG400, Polyethylene glycol 400; PMSF, phenylmethylsulfonyl fluoride; SDS, Sodium dodecyl sulfate; TNF-α, Tumor necrosis factor α; TRPV5, transient receptor potential vanilloid 5; TRPV6, transient receptor potential vanilloid 6; VEGF, Vascular endothelial growth factor.

Ca^{2+}-sensitivity and enhanced the rate constant of force re-development, which may also contribute to the enhanced survival rate in elderly mice.

KEYWORDS
aging, autophagy, klotho, rapamycin, senolytics

1 | INTRODUCTION

The present investigation is a continuation of efforts to characterize the underlying basis for the physical deterioration associated with normal multicellular aging, which includes painful and debilitating chronic diseases such as cardiovascular syndromes, cancer, and neurodegeneration.[1,2] A novel concept explored here is the capacity of rapamycin to increase expression of klotho protein as a correlate of increased survival of the drug-treated animals, along with autophagic biomarker proteins and other effects described here. The major focus of this work is the extent to which treatment of mice approaching the end of their normal expected median lifespan with rapamycin, an inhibitor of the serine threonine kinase mTOR, affects the survival of the animals and several critical indicators of age-related physical deterioration. Special attention is given to the effects of this treatment on expression of the Klotho gene, expression of which in mice correlates strongly with median lifespan and whole organism viability.[3] Previous research analyzing the klotho protein's influence on age-associated physical decline revealed that mice deficient in this molecule exhibited accelerated rates of aging.[4] Moreover, silencing Klotho expression was observed to dramatically increase the incidence of age-related diseases such as arteriosclerosis, osteoporosis, decreased physical activity, pulmonary emphysema, atrophy of skin, and muscle and impaired cognitive function. Moreover, decreased klotho levels were found in elderly mice leading to age-related cardiac complications including heart failure, hypertrophy, and remodeling, which were reverted by exogenous klotho.[5] Conversely, overexpression of klotho mediated increased life expectancy.[3,6]

Physical aging may be best described as an increasingly severe deterioration in organ function occurring in most animals once the peak reproductive timeframe has passed. Conceptually, this process may be most comprehensively visualized as a progressive shift in cellular phenotypes within each tissue of an individual to cells that either fail to contribute to organ function or disrupt healthy tissue and organ homeostasis. Aging also influences cardiac contractility at the cellular level via altering cardiac ion homeostasis and expression of contractile proteins.[7] Furthermore, recently enhanced cardiac aging was demonstrated in Klotho deficient mice, which was mediated by impaired autophagy.[8] Increasing the level of autophagy through mTOR inhibition is potentially a potent clinical tool for a wide range of disorders, as demonstrated, for example, by the success of Hyttinen et al. in reducing the severity of macular degeneration by rapamycin-mediated mTOR suppression and autophagy amplification in retinal cells of patients afflicted with the disorder.[9] Furthermore, inhibition of mTOR signaling by rapamycin was shown to suppress vascular calcification, in which upregulation of klotho was found to play a major role.[10] Based on the outcome of this and similar clinical evidence, the major working hypothesis for the present study is that treatment of mice with rapamycin will cause systemic mTOR suppression, with resulting general increases in autophagy. Further, it is expected that this treatment will cause "senolytic" effects—a reduction in senescent cell burden in each animal.

2 | MATERIALS AND METHODS

2.1 | Animals

Animals used in the present study were male C57Bl6 mice with an average weight of 42.5 ± 8.5 g. C57Bl/6 mice are commonly used in aging research, and males typically outlive females.[11-13] The age of these animals, based on information provided by the vendor (Charles River Laboratories), was between 650 and 750 days, with an average value of 24 months, an age range near the end of the observed median lifespan for this species, which may be extended by treatment with rapamycin.[14] Accordingly, within this report, the mice used for these experiments are designated "elderly." They were provided with standard rodent chow pellets (R/M-Z + H, ssniff Spezialdiäten GmbH, Soest, Germany) and water ad libitum and housed at an ambient temperature of 25 ± 2°C, with a relative humidity of 55% ± 5%, and a 12-h light–dark cycle. These housing conditions were selected as optimal for mice based on previous research by the authors using this model. Mice are known to thrive well at or slightly below their thermoneutrality range of ~29–32°C, which exceeds that of humans (~22°C).[15] All mice used in the present study had been acclimatized in the investigator's facility for at least 18 months prior to the initiation of the study.

2.2 | Treatment protocol, survival assessment, and biospecimen collection

Twenty-four-month-old C57BL male mice, were segregated into 2 groups of 7–8 animals each: a treatment group, members of which, beginning at 24 months, were administered 1.5 mg/kg rapamycin via interperitoneal (IP) injection once per week; and a control cohort, treated weekly with injection vehicle IP. Rapamycin (Tocris

Bioscience) was dissolved in ethanol as a stock solution of 15 mg/mL, then further diluted to 0.15 mg/mL in PBS containing 5% Tween-80, 5% PEG400, and 4% ethanol as described by Leontieva et al.[16] Treatment regimens were 12 weeks in duration. Body weight of mice was measured every week prior to the treatment. 8 days after the final injection of either rapamycin or vehicle, mice were anesthetized with an intraperitoneal pentobarbital sodium injection (60 mg/kg), and blood samples were obtained. After blood collection, under deep anesthesia, adipose tissue, brain, kidney, liver, muscle, lung, and heart were isolated and placed in liquid nitrogen. Blood and tissue samples were subsequently stored at −80°C. Molecular biological analyses is described below in the present report. Time course assessments of survival for each group of mice were conducted according to the methods of Harrison et al.[14] This experimental strategy as described by Harrison et al. was selected by authors of the present report as an optimal approach to providing solid preliminary data on rapamycin-mediated survival in this study.[15]

2.3 | Blood solute measurement

Following 12-week treatment with rapamycin or vehicle and prior to sacrifice, peripheral blood was collected from left external jugular vein of each animal using separator tube. After collection of the whole blood, it was allowed to clot by leaving it undisturbed at room temperature for 15 min. After that, it was centrifuged at 1500*g* for 15 min in a refrigerated centrifuge at 4°C. Mouse obesity enzyme-linked immunoassay (ELISA) Strip for profiling cytokines (Signosis Inc.) kit was used to determine the levels of leptin, TNF-α, IL-6, IGF-1, IL-1α, IL-1β, VEGF and MCP-1. Samples were applied in one strip of a 96 well plate and were incubated for 2 h at room temperature with gentle shaking. After 3 washings, 100 µL of diluted biotin-labeled antibody mixture was added to each well and incubated for 1 h at room temperature with gentle shaking. After 3 washings, 100 µL of diluted streptavidin-HRP conjugate were added to each well and incubated for 45 min at room temperature. Repeating the washing step, 100 µL of substrate was added to each well and incubated for 30 min. Then 50 µL of stop solution was added to each well, and the optical density of each well was determined with a microplate reader at 450 nm.

2.4 | Protein isolation

Approximately 100 mg of white adipose tissue, brain (cerebellum), kidney, muscle, lung, and heart (left ventricle) was lysed in 400 µL of isolating buffer (RIPA buffer containing 50 mM Tris–HCl, 1% NP-40, 0.5% Na-deoxycholate, 0.1% SDS, 150 mM NaCl, 2 mM EDTA, 50 mM NaF, 1 mM orthovanadate (a phosphatase inhibitor), 10 mM okadaic acid, 1 mM PMSF, and 1× protease inhibitor cocktail) using a polytron homogenizer. Homogenates were incubated for 60 min at 4°C. After that, they were centrifuged at 15142 g at 4°C for 10 min. The supernatant was transferred to a new tube. The protein concentration was determined by a BCA Protein Assay Kit (Thermo Scientific) using bovine serum albumin (BSA) as the standard. Samples were mixed with Laemmli buffer and boiled for 10 min.

2.5 | Western Blot analysis

Western blot analysis was carried out according to the Chemidoc Touch Imaging System protocol (Bio-Rad Laboratories). A total of 75 µg of protein from each sample were loaded and separated on 7.5% TGX Stain-Free gel for klotho (Bio-Rad Laboratories) and 12% TGX Stain-Free gel for p62 and LC3B-II. After separation, gels were exposed to UV light (thereby, trihalo compounds contained in stain-free gels covalently bind to tryptophan residues in proteins, allowing total protein quantification), and proteins were transferred to polyvinylidene difluoride (PVDF) membranes (Bio-Rad Laboratories, Hercules, CA, USA). After blocking the membranes with 5% nonfat dry milk in Tris-buffered saline with 0.1% Tween 20 (TBST) for 1 h, membranes were incubated with the primary antibody solution at 4°C overnight. Membranes were washed with TBST 3 times and incubated with horseradish peroxidase (HRP)-conjugated secondary antibody solution (1/2000, Cell Signaling Technology) for 1.5 h at room temperature. After washing, the membranes were developed using Clarify Western ECL Substrate (Bio-Rad Laboratories) and the optical density of the bands was measured by using the ChemiDoc Touch Imaging System. The expression of the protein of interest was normalized against the total amount of protein in each lane.[17,18] The results were evaluated by Image Lab 5.2.1 software (Bio-Rad Laboratories).

2.6 | Immunohistochemistry

The kidney samples were fixed in PBS buffered formaldehyde solution (4%) at pH 7.4 for 1 day. After that, samples were embedded in paraffin wax, and 4 um slides were made and deparaffinized using xylol and ethanol. Slides were treated with H_2O_2 (0.5%, 20 min) to inhibit endogenous peroxidase activity, then subjected to antigen retrieval in a buffer solution (pH 9.0, RE7119, Leica, Wetzlar, Germany). For immunohistochemistry, samples were incubated with Dako EnVision FLEX Peroxidase-Blocking Reagent (Dako, Glostrup, Denmark) for 5 min in a wet chamber, and washed with EnVision™ FLEX Wash Buffer. Antigen retrieval was performed in the epitope retrieval solution (RE-7119, Leica, Wetzlar, Germany) at pH 9.0 with a pressure cooker. Slides were then washed with distilled water and EnVision™ FLEX Wash Buffer. Samples were then incubated with Klotho (ab 154163, Abcam, USA) primary antibody at a dilution of 1:200 in EnVision™ FLEX Antibody Diluent at pH 6.0 for 1 h in a wet chamber at room temperature. Slides were then washed with EnVision™ FLEX Wash Buffer 3 × 5 min. The samples were then incubated with EnVision™ Flex+ Rabbit linker (15 min), and EnVision™ Flex/HRP enzyme (30 min) in the wet chamber followed by another washing step. Detection of antibody binding was achieved by incubation with the EnVision™ FLEX/HRP for 30 min, in the wet chamber

followed by another washing step. Slides were then incubated with DAB solution for 1–10 min (EnVision™ FLEX DAB+ Chromogen). Rinse in running tap water for 2–5 min. Dehydrate through 95% ethanol for 1 min, and 100% ethanol for 2×3 min. Clear in xylene for 2×5 min and cover with mounting medium. The intensity and distribution of immunostaining was assessed by light microscopy (Leica DM2500 microscope, DFC 420 camera, and Leica Application Suite V3 software, Leica).[19]

2.7 | Force measurement in permeabilized left ventricular cardiomyocytes

Force measurements were performed as described by Papp et al.[20] Briefly, frozen left ventricular (LV) tissue samples from control and rapamycin-treated mice were mechanically disrupted in isolating solution (ISO) (1 mM $MgCl_2$, 100 mM KCl, 2 mM EGTA, 4 mM ATP, 10 mM imidazole, pH 7.0) containing 0.5 mM phenylmethylsulfonyl fluoride, 40 μM leupeptin, and 10 μM E-64 protease inhibitors (Sigma-Aldrich). The mechanically isolated cardiomyocytes were incubated in ISO supplemented with 0.5% (v/v) Triton X-100 (Sigma–Aldrich) for 5 min at 4°C. Single permeabilized cells were attached with silicone adhesive (DAP 100% all-purpose silicone sealant) between two thin, stainless steel stylus ('insect') needles, connected to a sensitive force transducer (SensoNor, Horten, Norway) and an electromagnetic high-speed length controller (Aurora Scientific Inc.) in ISO at 15°C. Isometric force measurements were performed by transferring the cardiomyocytes from relaxing to activating solutions. The compositions of activating and relaxing solutions were calculated as described previously.[21] All solutions were supplemented with protease inhibitors (0.5 mM phenylmethylsulfonyl fluoride, 40 μM leupeptin, and 10 μM E-64 (Sigma-Aldrich). Ca^{2+} concentrations were estimated as −log10 [Ca^{2+}] (M) (pCa) units accordingly, the pCa of the activating and relaxing solutions was 4.75 and 9.0, respectively. At a given Ca^{2+} concentration, one contraction was measured in each myocardial cell. When testing stability, individual myocardial cells were activated at the beginning and end of the measurement series with the solution with the highest Ca^{2+} concentration (pCa = 4.75). During the evaluation of the measurement results, only those preparations were evaluated where, at the end of the experimental protocol, the maximum contractile force of the cell reached 80% of the initial value. The intermediate Ca^{2+} concentration (pCa 5.4) was calculated from the mixture of activating (pCa 4.75) and relaxing solutions (pCa 9.0) by a previously reported approximation.[21] Accordingly, pCa 4.75 corresponds to approx. 18 micromoles, pCa 6 corresponds to a concentration of about 1 micromol, and pCa 9 corresponds to 0 micromoles of Ca^{2+}. Each Ca^{2+}-activated contraction was followed by relaxation. Maximal Ca^{2+}-activated force ($F_{max,}$) was registered at pCa 4.75, while submaximal Ca^{2+}-activated force (F_{active}) was determined at intermediate [Ca^{2+}] (pCa 5.2–7.0) to construct pCa-force relationships. F_{active} values at intermediate [Ca^{2+}] were normalized to F_{max} (normalized F_{active}) and then fitted to a modified Hill equation (Origin 6.0, Microcal Software), creating a sigmoidal curve, to determine the Ca^{2+} sensitivity of the contractile machinery (pCa_{50}). The Ca^{2+}-independent passive force ($F_{passive}$) of cardiomyocytes was measured by shortening the preparations to 80% of their original lengths for 8 sec in relaxing solutions. The sarcomere length (SL) was adjusted to 2.3 μm; additionally, $F_{passive}$ was measured in relaxing solution. During single Ca^{2+} contractures, once the peak force was reached, the rate constant of force redevelopment ($k_{tr,max}$) was determined by a quick release–restretch maneuver in the activating solution. The original forces of every individual cell were normalized to myocyte cross-sectional-area, calculated by the width and height of the cardiomyocyte. Values of active or passive contractile force (F_{active} and $F_{passive,}$ respectively) were expressed as $F = kN/m^2$, as described by Fabiato et al[21]).

2.8 | Data analysis

All data were analyzed by GraphPad Prism version 7 (GraphPad Prism Software). The unpaired t-test was used for comparisons between two groups. For most of the data shown in this report, 2–4 measurements of a particular outcome were taken. Error bars on the figures represent the standard error of the mean (S.E.M.). The Kaplan–Meier method provided descriptive analysis of survival curves for the groups; survival curves were compared using log-rank tests.

Cardiomyocyte force generation was measured with a custom-built system (utilizing the DAQ platform produced by National Instruments) and recorded by a custom-built LabVIEW (National Instruments) module. Results were evaluated in Excel (Microsoft, 2007) and GraphPad Prism 5.0 (GraphPad Software). Error bars on the figures represent the standard error of the mean (S.E.M.). The values presented in this study were expressed as mean ± S.E.M. Statistical significance was calculated by an unpaired t-test. The level of statistical significance was $p < 0.05$.

3 | RESULTS

3.1 | Effect of rapamycin treatment on 12-week survival of elderly mice, and bodyweight

Figure 1A shows a comparison of the percentage of elderly mice in the group treated by IP injection with 1.5 mg/kg/week rapamycin versus the group of control animals receiving injection vehicles. As displayed, 43% of the control animals died during the 12-week evaluation period, whereas all of the rapamycin treated mice survived. As shown in Figure 1B, during the 12-week treatment period, the rapamycin-treated mice experienced a weight loss that was small but significantly more than the average weight lost by control animals ($p < 0.05$). At the outset of the treatment period, 7 animals were present in the vehicle-treated control group, decreasing to 4 surviving animals after 12 weeks. Eight mice were present in the rapamycin group, all of which survived for 12 weeks.

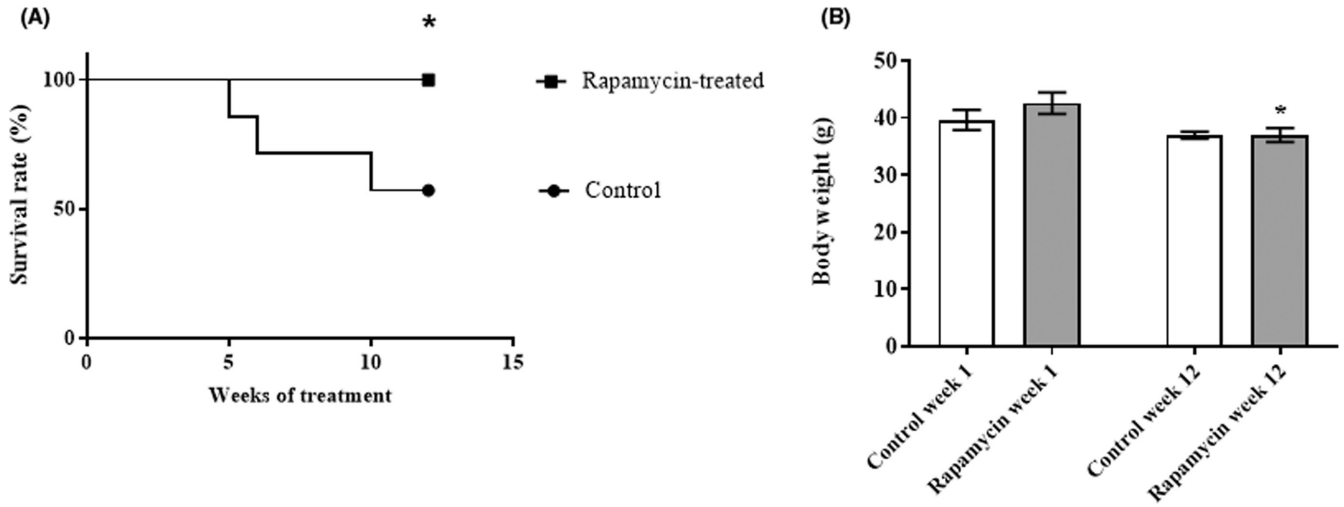

FIGURE 1 Effect of injected rapamycin on the survival of elderly mice, and body weight. The Kaplan–Meier assessment protocol was used during a 12-week period to evaluate the effect on survival of a test group of 24-month-old C57BL6 mice, treated once weekly with 1.5 mg/kg rapamycin injections IP ($n=8$), versus a group of control animals administered IP administration of injection vehicle ($n=7$). Data outcomes are shown as the percentage of animals alive from each of the 2 groups at selected time points (A). Average body weight is shown in (B). Results are expressed as mean ± SEM. $n=4$ in control. $n=8$ in rapamycin-treated group. $^*p<0.05$ in comparison with the control group.

3.2 | Rapamycin effect on humoral mediators of immune activity

Figure 2 shows the effect of IP rapamycin injections (one per week for 12 weeks) in elderly mice on serum content of immunoactive proteins such as leptin, TNF-α, IL-6, IGF-1, IL-1α, IL-1β, VEGF, and MCP-1 were evaluated using cytokine ELISA analysis of whole blood serum from the mice. Data outcomes of this experiment, shown in Figure 2, demonstrated that although no statistically significant differences in the content of any of the 8 solute molecules were detected, a nonsignificant trend toward levels of leptin (2A), IL-6 (2C), IL-1α (2E), TNF-α (2B), IL-1β (2F), and IGF-1 (2D) slightly decreased in the serum of rapamycin-treated mice versus controls was observed; moreover, a nonsignificant trend toward slightly elevated serum levels of VEGF (2G), MCP-1 (2H) and in rapamycin-treated mice versus control animals was also seen, as shown in Figure 2.

3.3 | Influence of rapamycin on Klotho protein expression in liver, kidney, lung, muscle, adipose, brain, and heart tissue

Western blot data shown in Figure 3 depicts klotho protein content in selected tissues from elderly (24-month-old) C57BL6 mice, either treated with 1.5 mg/kg rapamycin or vehicle via intraperitoneal (IP) injection once per week; for 12-week time course regimens. Klotho protein expression in samples from rapamycin-treated mice was observed to significantly exceed klotho content in control mice for kidney ($p<0.001$; Figure 3A); adipose ($p<0.005$; Figure 3B); brain ($p<0.005$) (Figure 3E) and heart ($p<0.05$) (Figure 3F). Figure S1 shows immunohistochemical staining of klotho protein in kidney obtained from treated and control animals.

3.4 | Effect of rapamycin treatment on autophagy-related proteins in selected tissues

Figure 4 shows Western blot evaluation of selected tissues from rapamycin-treated, versus vehicle-treated control mice for the content of the apoptosis-associated proteins p62 and LC3B-II. The major findings include an observation of significantly elevated levels of LC3B-II in adipose tissue and kidney from rapamycin-treated mice (Figure 4A,B); and a rapamycin treatment reduction in adipose tissue and kidney expression of p62 relative to that in the same tissues of vehicle-treated control mice (Figure 4A,B) ($p<0.05$). Rapamycin treatment enhanced the level of LC3-II and decreased p62 in heart and brain, however, it did not reach a significant level.

3.5 | Effect of rapamycin treatment on cardiomyocyte contractility

To determine the effect of rapamycin on myofilament protein function Ca^{2+}-activated, active (F_{active}), Ca^{2+}-independent, passive force ($F_{passive}$), Ca^{2+}-sensitivity of isometric force production (pCa_{50}), and the rate constant of force redevelopment at the maximal level of Ca^{2+} activation ($k_{tr,max}$) were measured in left ventricular permeabilized cardiomyocytes. Measurements were taken at a sarcomere length of 2.3 micrometers because this corresponds to the physiological sarcomere length.[22] The precise adjustment of the sarcomere lengths was performed using a video microscopy system, which allows the sarcomere length to be accurately measured by selecting the entire myocardial cell. F_{active} values in rapamycin-treated animals did not differ from those of drug-treated mice and vehicle-treated control animals. Moreover, $F_{passive}$ did not differ between the control and rapamycin-treated groups, either. The above results are illustrated in

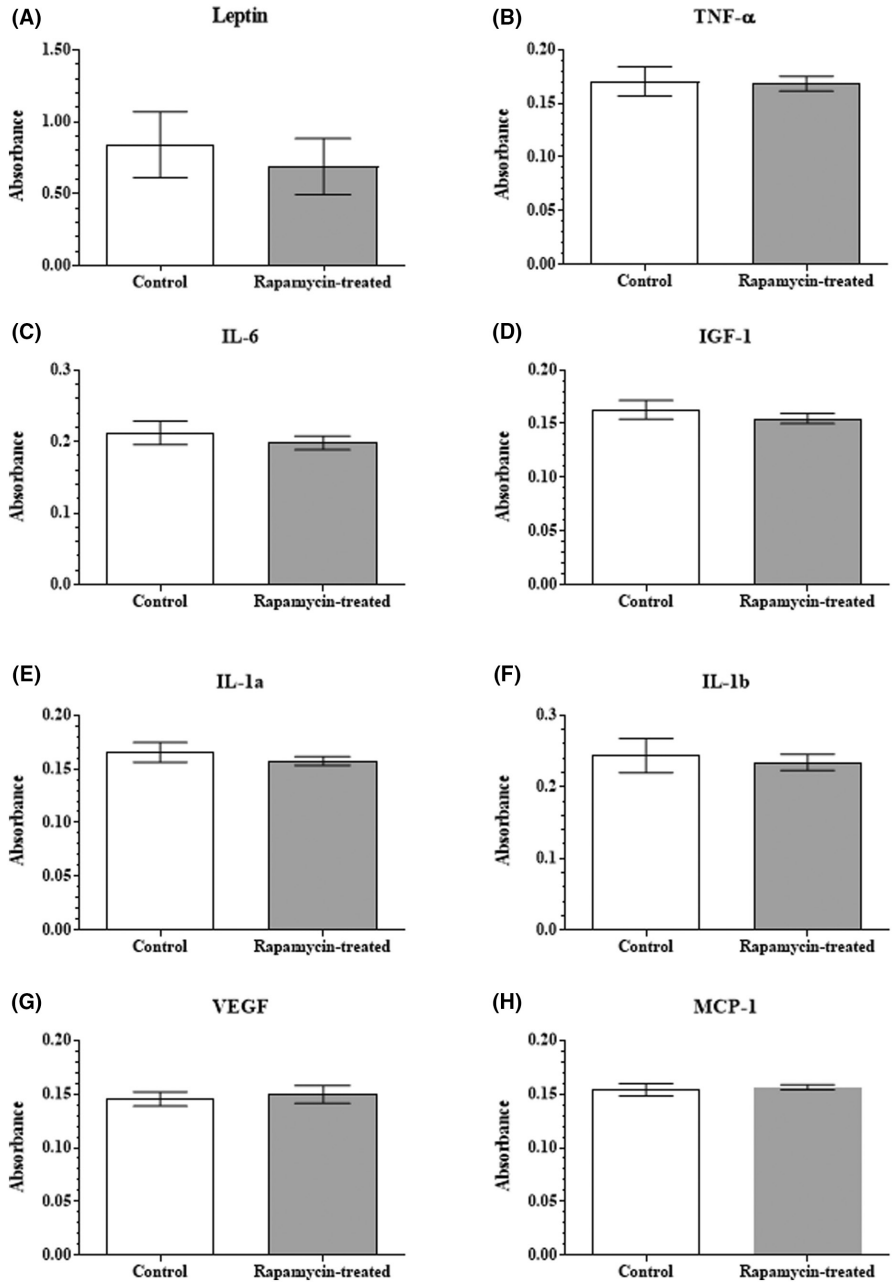

FIGURE 2 Effect of rapamycin treatment on the serum content of humoral immune mediators in peripheral blood of elderly mice. Whole blood serum obtained through centrifugation and clot expression, was assayed by ELISA for the immunoactive proteins leptin (A), TNF-a (B), IL-6 (C), IGF-1 (D), IL-1a (E), IL-1b (F), VEGF (G), and MCP-1 (H). Serum content of each protein is here displayed graphically as relative absorbance units at 450 nm expressed as mean ± SEM for serum from the test and control groups ($n = 4–8$).

Figure 5A–D, in detail. Nevertheless, pCa_{50} was higher in cardiomyocytes isolated from hearts in the rapamycin-treated group than in vehicle-treated control animals (Figure 5E). Additionally, $k_{tr,max}$ was significantly higher in the rapamycin treated group than in controls (Figure 5F).

4 | DISCUSSION

The data shown here constitutes a starting point for examining the relationship between klotho activity and autophagy as a component of age-associated physical deterioration. Findings reported here and by other investigators raise the possibility of potential exploitation of the bioactive properties of klotho in future strategies for prevention and therapy of age-associated pathologies. Moreover, recent demonstrations of cardio protection through induction of increased klotho expression[23] underscore the potential clinical value of research initiatives such as the effort on which the present report is based, which expand understanding of the klotho protein and its possible preventive and therapeutic applications in the future. Indeed, the findings described here offer potentially enormous clinical applications in the future development of rapamycin and klotho as increasingly versatile tools in the management of age-associated chronic illness and in possible life extension strategies. It is nevertheless important to understand that this prediction is subject to a significant caveat regarding the clinical use of the Klotho gene product. The Klotho gene encodes α, β, and Klotho-related proteins.[24] The extracellular domain of α-Klotho may be cleaved to release a soluble form into blood, urine, and cerebrospinal fluid, where it exerts its biological function as a humoral factor with weak ß-glucoronidase

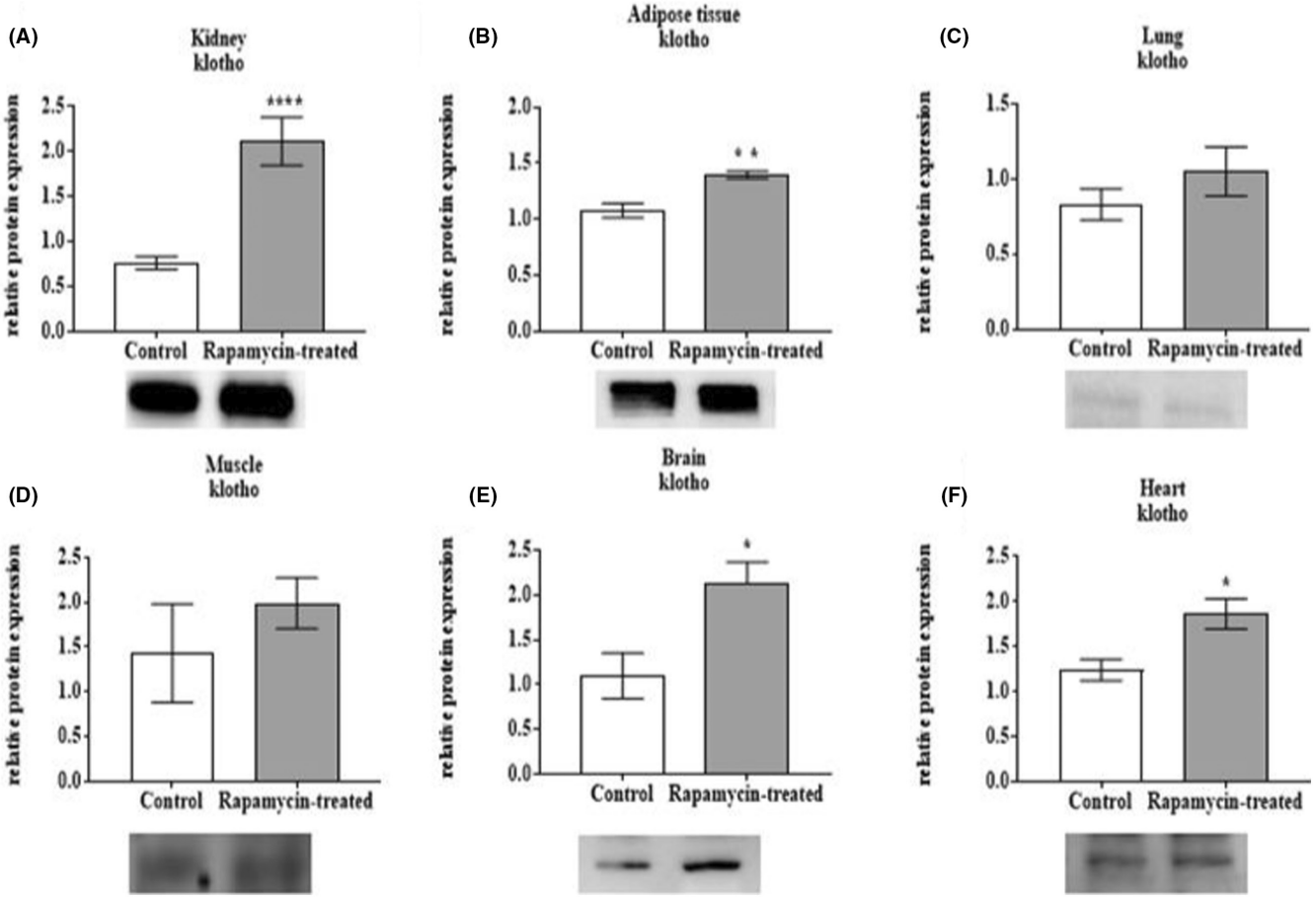

FIGURE 3 Influence of rapamycin on tissue-specific klotho protein expression. Western blot was used to detect expression of klotho protein, shown as the dependent variable in each graph in this figure as relative protein units. A comparison of klotho protein content of tissue from rapamycin-treated, versus vehicle-treated mice is shown for the kidney (A), adipose tissue (B), lung (C), skeletal muscle (D), brain (E), and heart (F); and $^{*}p < 0.05$ $^{**}p < 0.01$ $^{***}p < 0.001$ in comparison of klotho expression in selected tissues from rapamycin-treated mice versus the control group.

and sialidase activity and is an activator of TRPV5 and TRPV6 ion channels. It also inhibits growth factor signaling and oxidative stress. Additionally, the Klotho gene product exists as a type-I membrane protein that regulates the inflammatory response through interaction with the transcription factor nuclear factor-kappa beta (NF-kB) proteins, with overexpression observed to extend vertebrate life span through modulation of the insulin/insulin-like growth factor-1 (IGF-1) signaling pathway.[25] Recently, researchers reported that Klotho exhibited a potent ability to suppress potentially pathological apoptotic depletion of cardiac cells. Klotho protein was observed to mediate this effect through induction of the heat shock protein (hsp) 70 gene, with downstream inhibition of caspase-3 activation, increased expression of the pro-survival proteins Bcl-2, phosphorylated (p-)Akt, and Bad, and concomitantly reduced expression of the pro-apoptotic protein Bax.[26] Findings of the present investigation with potential relevance to the development of improved strategies for the management of diseases in which autophagic activity plays a role, include an observation of significantly elevated levels of LC3B-II in adipose tissue and kidney from rapamycin-treated mice and a reduction in rapamycin treatment in adipose tissue and kidney expression of p62 relative to that in the same tissues of vehicle-treated control mice. Furthermore, similar trends were observed in the heart and brain. The critical relevance of p62, LC3B-II, and other regulators and biomarkers for autophagic processes is based on the (mostly) reciprocal relationship autophagy has with the underlying cellular and molecular pathogenesis exhibited by diseases of old age. Autophagy is the major countermeasure evolved by cells to defend against this process and is significantly diminished with advancing age.[27,28] Accordingly, increased autophagy participates in the removal of damaged and toxic proteins and organelles and protects against age-related chronic disease.[29,30]

Outcomes showing a rapamycin treatment-associated increase of LC3B-II in adipose tissue and kidney, indicate that autophagic activity in these tissues is indeed augmented by rapamycin treatment. Moreover, high levels of klotho protein expression by the kidney, also increased by rapamycin, suggest the existence of some (as yet undefined) mechanism by which klotho may participate in the induction of autophagy. The existence and nature of such a mechanism are speculative and constitute a major objective of the ongoing aging research by authors of this article.

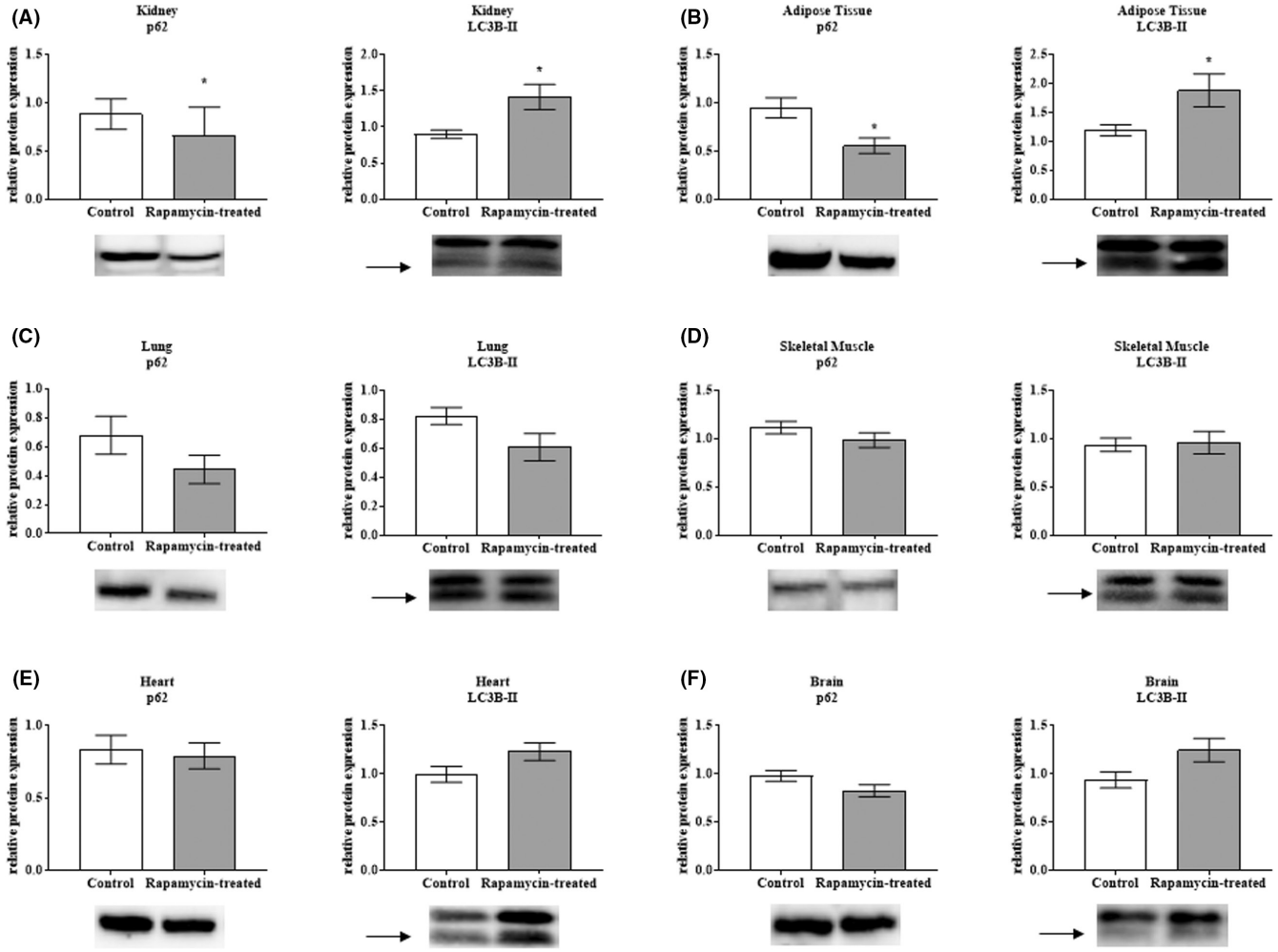

FIGURE 4 Influence of rapamycin on tissue-specific expression of apoptotic proteins p62 and LC3B-II. Western blot was used to detect expression of apoptosis-associated proteins p62 and LC3B-II. Amounts of these proteins in selected tissues is shown as the dependent variable in each graph in this figure as relative protein units estimated based on Western blot results. Comparison of p62 and LC3B-II protein content of tissue from rapamycin-treated, versus vehicle-treated mice is shown for kidney (A) adipose tissue (B), lung (C), skeletal muscle (D), heart (E), and brain (F). Relative protein content of tissues were normalized to the total protein level. $^{*}p < 0.05$ in comparison of p62 and LC3B-II expression in selected tissues from rapamycin-treated mice versus the control group.

Also intrinsic to these broad objectives is an analysis of how rapamycin affects cardiac myofilament function. The present investigation demonstrated, that although experiments conducted in the present study, failed to demonstrate significant enhancement of cardiomyocyte contractility, as shown in Figure 5. Nevertheless, rapamycin treatment increased pCa50, as shown in Figure 5E. This outcome confirmed findings by Brenda Schoffstall et al. in their evaluation of the capacity of rapamycin to modulate cardiac and skeletal muscle contraction.[31] A further major outcome of the present investigation is the demonstration that rapamycin treatment significantly increased the rate constant of muscle force redevelopment (ktr, max). Nevertheless, it was also observed that rapamycin treatment did not alter $F_{passive}$. Recently, Boldt and colleagues have shown a gradual increment in calcium sensitivity during the maturation of SD-rats.[32] Earlier, results suggested decreased calcium sensitivity in myocytes obtained from rats with advanced age.[33] These results indicate that calcium sensitivity may be described by a parabola. Our results suggest that rapamycin and enhanced klotho expression can enhance calcium sensitivity and improve myofilament function in advanced age, which may contribute to enhanced survival.

In conclusion, based on the results of the work described here, this effect may exhibit a strong positive correlation with enhanced survival in the drug-treated group. Similar findings have been reported earlier.[14] Key findings of the present study also include observations that rapamycin treatment exerted a minor but significant inhibition of body weight gain; A particularly interesting outcome of this investigation is the rapamycin treatment-associated increase in klotho protein expression shown by Western blot. Figure 4 shows that levels of the apoptosis-associated proteins p62 and LC3B-II may be significantly modulated by rapamycin treatment in different tissues. Finally, assessment of rapamycin's effects on cardiomyocyte contractile force demonstrates that this outcome may also be modulated by the drug, thus offering future potential for its expanded use in cardiovascular medicine.

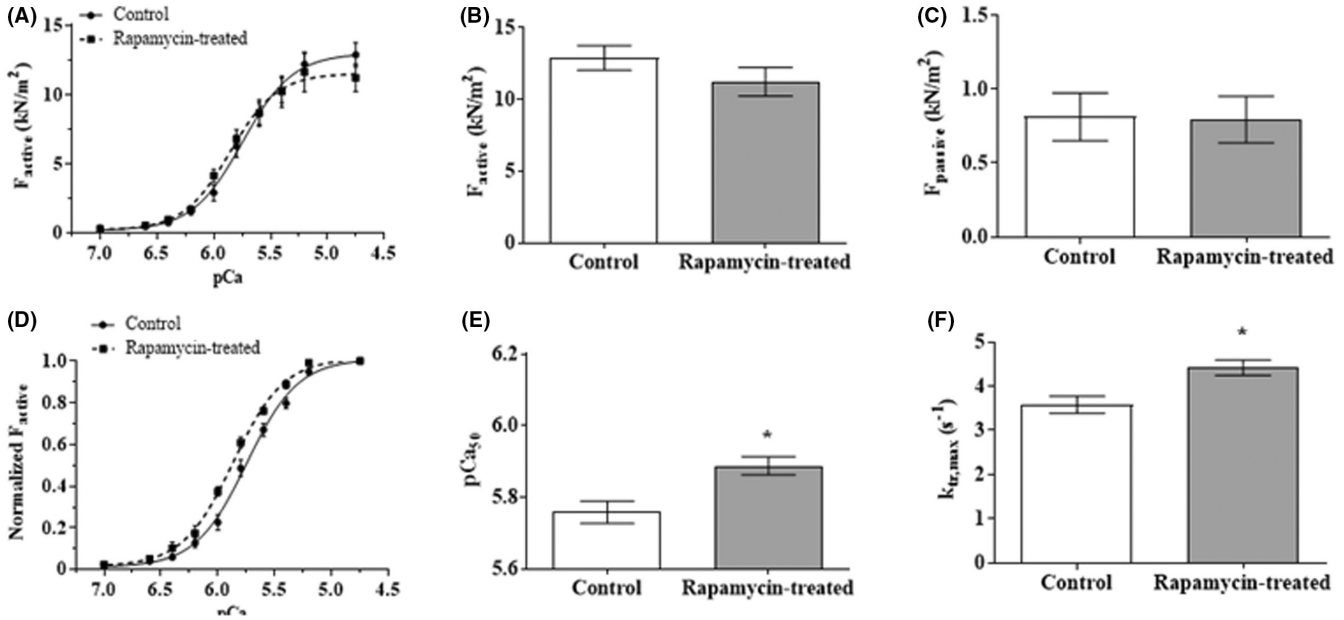

FIGURE 5 Rapamycin treatment effects on cardiomyocyte force production. (A) shows active force in kilonewtons per square meter (F_{active}, kN/m^2) at selected concentrations of calcium ions for rapamycin-treated and vehicle-treated (control) mice. [Ca^{2+}] is expressed as pCa (–log [Ca^{2+}] in units of M). The relative active contractile force (F_{active} (kN/m^2) exerted by cardiomyocytes from vehicle-treated control mice versus those receiving rapamycin injections at an arbitrarily selected (representative) pCa of 5.25 is displayed in (B), and a comparison of passive contractile force ($F_{passive}$ (kN/m^2)) exerted by cells from vehicle-injected control mice, versus those treated with rapamycin at a pCa^{2+} of 5.25 is shown in (C). The Origin 6.0, Microcal Software was used with normalized F_{active} values to create a sigmoidal curve for the determination of the Ca^{2+}-sensitivity of force production (pCa_{50}) (D). pCa_{50} was considered the [Ca^{2+}] generating half maximal force (E), and the rate constant of force redevelopment ($k_{tr,max}$) at maximal activation was determined following rapid release and re-stretch (F). Data were obtained from cardiomyocytes of vehicle-treated control mice (white columns), and of rapamycin-treated mice (shaded columns). Results of measurements in cardiomyocytes from rapamycin-treated animals are expressed as mean ± SEM. $^*p < 0.05$ in comparison with cardiomyocytes from vehicle-treated control mice.

5 | LIMITATIONS

In summary, a major objective of this investigation and its unique value to ongoing exploration of the underlying features of the aging process is that this study provides preliminary insight into how rapamycin affects klotho protein expression in the organs studied here – since klotho is also known to mediate processes that affect normal aging.[3,6] Here, the investigators structured this initial evaluation of rapamycin'seffects on klotho within the same investigative venue as an evaluation of rapamycin's effects on the expression of proteins involved in regulation of autophagy. The rationale for grouping these topics within a single small study is that autophagy is a process that is intrinsic to cellular senescence and is promoted by rapamycin-mediated inhibition of mTOR (Haines et al, 2013,[27]), making a simultaneous comparison of rapamycin effects on both autophagy and klotho useful for ongoing and future research. The study on which this report is based was small and preliminary and did not seek to define specific cellular and molecular details of processes contributing to senescence. Continuing research by the authors into pharmacological intervention in mTOR-dependent aspects of cellular and whole-organism senescence will build on the investigative paradigm used here, while acknowledging that aspects of the original experimental design limited the breadth of conclusions that may be drawn from data outcomes shown here. Seven major limitations on use of this report as an information source—and approaches for overcoming these limitations in future investigation of rapamycin effects on age-related processes are summarized as follows: (1) Rapamycin-associated suppression of body weight gain shown in Figure 1 did not incorporate relative total fat mass measurements. (2) Male C57Bl/6 mice typically outlive females – which influenced the model selection for these experiments. Future studies will nevertheless evaluate the influence of sex differences on study outcomes. (3) Three animals from the control group died. No gross evidence of lethal pathology was noted, however no autopsies were performed—resulting in some ambiguity of outcome. (4) In the present study, the investigators typically made 2–4 measurements for each outcome displayed and independent t-tests to were used to determine significance. For future studies in the same range of sample size as was utilized in this investigation, nonparametric statistics would be more appropriate. (5) It is here acknowledged that description of time course data outcomes of this study, such as survival of elderly animals would have benefitted by correlation with monitoring of senescent cells. Nevertheless, despite limitations imposed by constraints on sample size and range of testing, the basic objective of the study was achieved. Specifically, it was demonstrated that rapamycin treatment of the elderly mouse population utilized, did in fact correlate with enhanced survival of the treated, versus control mice—along with changes in senescence- and autophagy-associated

biomarkers consistent with senolytic outcomes. (6) mTOR signaling was not measured in the present investigation. Assessment of the effects of inhibition of this enzyme by rapamycin would have been useful. (7) Senescent cell representation in tissue was not measured in the present investigation, a limitation which constrains interpretation of rapamycin effects on a major driver of age-associated physical deterioration for each of the tissues examined.

AUTHOR CONTRIBUTIONS

For research articles with several authors, a short paragraph specifying their individual contributions must be provided. The following statements should be used "Conceptualization, Donald David Haines, and István Lekli; methodology, Kitti Szőke, Beáta Bódi, Zoltán Hendrik, Alexandra Gyöngyösi and Attila Czompa; validation Zoltán Papp, Donald David Haines, Árpád Tósaki, and István Lekli; resources, Zoltán Papp, Árpád Tósaki, and István Lekli; data curation, Kitti Szőke, Beáta Bódi, Attila Czompa, and Alexandra Gyöngyösi; writing—original draft preparation, Kitti Szőke and Donald David Haines; writing—review and editing, Zoltán Papp, Árpád Tósaki, and István Lekli. All authors have read and agreed to the published version of the manuscript."

FUNDING INFORMATION

This study was supported by NKFI-143360, GINOP-2.3.4-15-2020-00008, EFOP-3.6.3-VEKOP-16-2017-00009, EFOP-3.6.1-16-2016-00022 projects. The project is co-financed by the European Union and the European Regional Development Fund. The research was supported by the Thematic Excellence Program (TKP2020-IKA-04) of the Ministry for Innovation and Technology in Hungary.

CONFLICT OF INTEREST STATEMENT

The authors declare no conflict of interest.

DATA AVAILABILITY STATEMENT

The data presented in this study are available on request from the first or corresponding author.

INSTITUTIONAL REVIEW BOARD STATEMENT

All animals received humane care in compliance with the "Principles of Laboratory Animal Care" (formulated by the U.S. National Society for Medical Research, as described in U.S. National Institutes of Health publication No. 86–23, revised 1996) and the "Guide for the Care and Use of Laboratory Animals." Maintenance and treatment of animals used in the present study was additionally approved by the Institutional Animal Care and Use Committee of the University of Debrecen, Debrecen, Hungary (3/2012/DEMAB)

ORCID

Kitti Szőke https://orcid.org/0000-0001-6254-524X

REFERENCES

1. Ilaria B, Paul PK. Modelling ageing and age-related disease. *Drug Discov Today Dis Model*. 2016;20:27-32.
2. Niccoli T, Partridge L. Ageing as a risk factor for disease. *Curr Biol*. 2012;22:R741-R752.
3. Kuro-o M. Klotho and aging. *Biochim Biophys Acta*. 2009;1790:1049-1058.
4. Hu MC, Shi M, Zhang J, et al. Klotho deficiency causes vascular calcification in chronic kidney disease. *J Am Soc Nephrol*. 2011;22:124-136.
5. Chen K, Wang S, Sun QW, Zhang B, Ullah M, Sun Z. Klotho deficiency causes heart aging via impairing the Nrf2-GR pathway. *Circ Res*. 2021;128:492-507.
6. Kurosu H, Yamamoto M, Clark JD, et al. Suppression of aging in mice by the hormone klotho. *Science*. 2005;309:1829-1833.
7. Feridooni HA, Dibb KM, Howlett SE. How cardiomyocyte excitation, calcium release and contraction become altered with age. *J Mol Cell Cardiol*. 2015;83:62-72.
8. Li-Zhen L, Chen ZC, Wang SS, Liu WB, Zhuang XD. Klotho deficiency causes cardiac ageing by impairing autophagic and activating apoptotic activity. *Eur J Pharmacol*. 2021;911:174559.
9. Hyttinen JM, Petrovski G, Salminen A, Kaarniranta K. 5′-adenosine monophosphate-activated protein kinase–mammalian target of rapamycin Axis As therapeutic target for age-related macular degeneration. *Rejuvenation Res*. 2011;14:651-660.
10. Zhao Y, Zhao MM, Cai Y, et al. Mammalian target of rapamycin signaling inhibition ameliorates vascular calcification via klotho upregulation. *Kidney Int*. 2015;88:711-721.
11. Kohzaki M, Ootsuyama A, Umata T, Okazaki R. Comparison of the fertility of tumor suppressor gene-deficient C57BL/6 mouse strains reveals stable reproductive aging and novel pleiotropic gene. *Sci Rep*. 2021;11:12357.
12. So EY, Jeong EM, Wu KQ, et al. Sexual dimorphism in aging hematopoiesis: an earlier decline of hematopoietic stem and progenitor cells in male than female mice. *Aging (Albany NY)*. 2020;12:25939-25955.
13. Zhu WS, Naler L, Maul RW, Sallin MA, Sen JM. Immune system development and age-dependent maintenance in klotho-hypomorphic mice. *Aging (Albany NY)*. 2019;11:5246-5257.
14. Harrison DE, Strong R, Sharp ZD, et al. Rapamycin fed late in life extends lifespan in genetically heterogeneous mice. *Nature*. 2009;460:392-395.
15. Seeley RJ, MacDougald OA. Mice as experimental models for human physiology: when several degrees in housing temperature matter. *Nat Metab*. 2021;3:443-445.
16. Leontieva OV, Paszkiewicz GM, Blagosklonny MV. Weekly administration of rapamycin improves survival and biomarkers in obese male mice on high-fat diet. *Aging Cell*. 2014;13:616-622.
17. Gurtler A, Kunz N, Gomolka M, et al. Stain-free technology as a normalization tool in Western blot analysis. *Anal Biochem*. 2013;433:105-111.
18. Mizushima N, Yoshimori T. How to interpret LC3 immunoblotting. *Autophagy*. 2007;3:542-545.
19. Gall T, Petho D, Nagy A, et al. Heme induces endoplasmic reticulum stress (HIER stress) in human aortic smooth muscle cells. *Front Physiol*. 2018;9:1595.
20. Papp Z, Szabo A, Barends JP, Stienen GJ. The mechanism of the force enhancement by MgADP under simulated ischaemic conditions in rat cardiac myocytes. *J Physiol*. 2002;543:177-189.
21. Fabiato A, Fabiato F. Calculator programs for computing the composition of the solutions containing multiple metals and ligands used for experiments in skinned muscle cells. *J Physiol Paris*. 1979;75:463-505.
22. de Tombe PP, ter Keurs HE. The velocity of cardiac sarcomere shortening: mechanisms and implications. *J Muscle Res Cell Motil*. 2012;33:431-437.
23. Olejnik A, Franczak A, Krzywonos-Zawadzka A, Kaluzna-Oleksy M, Bil-Lula I. The biological role of klotho protein in the development of cardiovascular diseases. *Biomed Res Int*. 2018;2018:5171945.

24. Xu Y, Sun Z. Molecular basis of klotho: from gene to function in aging. *Endocr Rev*. 2015;36:174-193.
25. Di Bona D, Accardi G, Virruso C, Candore G, Caruso C. Association of Klotho polymorphisms with healthy aging: a systematic review and meta-analysis. *Rejuvenation Res*. 2014;17:212-216.
26. Hu J, Su B, Li X, Li Y, Zhao J. Klotho overexpression suppresses apoptosis by regulating the Hsp70/Akt/bad pathway in H9c2(2-1) cells. *Exp Ther Med*. 2021;21:486.
27. He LQ, Lu JH, Yue ZY. Autophagy in ageing and ageing-associated diseases. *Acta Pharmacol Sin*. 2013;34:605-611.
28. Rubinsztein DC, Marino G, Kroemer G. Autophagy and aging. *Cell*. 2011;146:682-695.
29. Glick D, Barth S, Macleod KF. Autophagy: cellular and molecular mechanisms. *J Pathol*. 2010;221:3-12.
30. Metcalf DJ, Garcia-Arencibia M, Hochfeld WE, Rubinsztein DC. Autophagy and misfolded proteins in neurodegeneration. *Exp Neurol*. 2012;238:22-28.
31. Schoffstall B, Kataoka A, Clark A, Chase PB. Effects of rapamycin on cardiac and skeletal muscle contraction and crossbridge cycling. *J Pharmacol Exp Ther*. 2005;312:12-18.
32. Boldt K, Joumaa V, MacDonald G, Rios JL, Herzog W. Cardiac ventricular muscle mechanical properties through the first year of life in Sprague-Dawley rats. *Mech Ageing Dev*. 2020;192:111359.
33. Wahr PA, Michele DE, Metzger JM. Effects of aging on single cardiac myocyte function in Fischer 344 x Brown Norway rats. *Am J Physiol Heart Circ Physiol*. 2000;279:H559-H565.

SUPPORTING INFORMATION

Additional supporting information can be found online in the Supporting Information section at the end of this article.

How to cite this article: Szőke K, Bódi B, Hendrik Z, et al. Rapamycin treatment increases survival, autophagy biomarkers and expression of the anti-aging klotho protein in elderly mice. *Pharmacol Res Perspect*. 2023;11:e01091. doi:10.1002/prp2.1091